Response letter

Dear Editor and reviewer,

We would like to show our sincere thanks to your time and efforts devoted to this work. We carefully read and made changes to all raised comments. Please find the point-by-point reply to each specific comments below.

5

Comments from the Editor:

Dear authors, your article needs to be further improved in some sections. Please check carefully the minor-moderate comments raised by one reviewer, and provide suggested changes. In addition, I recommend a check on the figures since scale bars in some are missed. Quantification of errors seems also missed.

10   I will provide a final editorial check after the above-suggested changes.

Response: Thanks for this editorial comments. We re-checked all figures and added scale bars in Figure 2b, Figure 3 and Figure 5.

To make quantifications of errors clear, we re-wrote the sub-section "*2.2.2 Error Assessment and postprocessing*".
15   Uncertainties in this work were quantified in two parts. For every image pair, "…*Standard deviations of displacements within the stable zone shows uncertainties, which can be used an index to show the quality of the derived results for a given image pair…*" (lines 104-106). In addition, "*In this work, we cross-validated measured slope displacements for five target images in 2019 in the second step. Uncertainties of the slope displacements for a given target image are estimated from all 19 base images in the stable periods. Standard deviations of these 19 measurements were used to indicate their reliability*" (lines 108-
20   110). In the results, quantifications of errors were shown in Figure 3, Figure 4 and Table 3. As we have mentioned in sub-section 2.2.2, uncertainties in this work have been shown in two ways: 1) standard deviations of displacements in the stable zone is used as uncertainties of a single image pair (such as Table 3), and 2) standard deviations of derived displacements from 19 image pairs in "*the second step*" are uncertainties for a given target image by using 19 base images in the stable period (Figure 3 a2, b2, c2, d2 and e2 and vertical bars in subpanels p1-p6 of Figure 4).

25

Report #2

I have genuinely appreciated the manuscript. I think the text is clear and informative enough in terms of technical details
30   (although I should say that a traditional methodological section is not featured in the text and I should leave the judgement on whether this is appropriate or not to other reviewers).
The figures are also quite nicely displayed, notations are correct and the content well agrees with the results reported in the text.

Overall, I have quite a positive feedback on the manuscript. However, I feel there are few things that can still be substantially improved.

1. For instance, I find the discussions and conclusions to be lacking from the interpretive standpoint. I would definitely suggest adding a few subsections in the discussion part (quite short and essential right now). In this sense, you could definitely invest more efforts in putting your contribution in context with respect to the current literature. In this way, you could emphasize how different is the work you present as well as potential strengths and weaknesses.

Response: Thanks for this comments. We added a few paragraphs and subtitles in the discussion part to put this work in context with the current literature. We compared the difference of the image correlation method used in this work with InSAR in the subsection "4.2 Comparison of image matching and InSAR methods". In this part, strength and weakness of the method is discussed. Please refer to lines 167-195 of the revised manuscript for details. For the first paragraph, we briefed the principles of both types of methods and pointed out that they are excel at detecting different deformation scales. The influences of temporal interval within an image pair, vegetation and mountain terrains are discussed in the following three paragraphs.

2. Also, I find the discussions to be lacking on the operational side of the work you present. You could talk to the NHESS readership and mention if you think the procedure you present to be applicable elsewhere. And if yes (which should be the case), what are the complexity one may face in repeating the same analytical protocol.
   To explain a bit further what I meant above, I have found the text to be mentioning monitoring activities only twice and mostly as a minor comment. However, I feel the technique you present to be very well versed for monitoring purposes. Assuming this to be true, then you could open up a small discussion on what type of monitoring can actually be done. Could you monitor all types of landslides? In the study area section, you could provide a better description of the landslide you analyzed. Please consider that the NHESS readership, as your manuscript is right now, has to wait until Section 2.3 to understand what type of landslide you have worked on. And you just use the following sentence: "Evidenced by optical images, the landslide in this work is a translational type and could be dealt with in this way (Highland and Bobrowsky 2013)". By adding more on the landslide description, you could also call again on this topic in the discussion and mention what type of landslides would be equally recognizable in your multi-temporal displacement estimation? Also, are every environment equally good to support this type of analyses? You mentioned that you initially used the red band because it is less sensitive to atmospheric effects and vegetation cover. Would it be possible to use the same technique in a less vegetated area? Or would you rather use another band in such cases? Also, what if the vegetation would be even denser than the study area you chose? Would your approach be equally successful? I think that these are the type of questions that the readership of NHESS would appreciate potentially even more than the technical side of the manuscript you present.
   This is exactly the point I am trying to raise here. As the manuscript is structured, it feels more like a technical note rather than a research article. My suggestion is to care for the interpretative and story-telling side of your research as much as

you did for the technical and method-specific part, which I think you did a good job at describing (although my expertise
70   does not really fall into optical remote sensing).
        Please try to consider my suggestions and add a more general or generalizable flavor to your article. Then, I think it would
        be a nice and complete contribution to read.

Response: Thanks for this insightful and detailed comments. Changes were made on the discussion and method parts of the
75   manuscript. We grouped your comments on two major sides, one related to vegetation and one related with landslide types.
        These two sides also cover other related issues such as situations that the audience of the *NHESS* may face.

To the questions of vegetation's influence:

        We discussed the impact of vegetation density on the method in lines 181-184. "*Both methods works well on bare land*
80   *without vegetation, though dense vegetation could seriously affect InSAR methods (Intrieri et al. 2018). On the contrary, image*
        correlation methods are less affected by vegetation cover as long as both images in a pair are from the same seasons (Yang
        2020). As image correlation methods use pattern matches within an image pair, we speculate that vegetation density may not
        a major challenge on derived results."

        We discussed why we select the red band in the Sentienl-2 images and whether other bands are applicable in lines
85   184-189: "*The Sentinel-2 images used in this work have four 10-metre resolution optical bands (Gascon et al. 2017). In theory,*
        any of these four bands may be used to derive slope displacements. But an ideal band should not be sensitive to ground cover
        change unrelated with ground displacements, which could minimize background noises. In general, optical bands with shorter
        wavelength is more prone to be affected by moisture in the atmosphere. Considering that near infrared band is very sensitive
        to vegetation, we used the red band in this work."

90

To the questions of landslide types:

        Potential applications to other types of landslides are discussed in the new added subsection "*4.4 Potential*
        applications of the method in landslide monitoring". In addition, we added a few sentences in the method part to describe the
        type of this imminent landslide in lines 66-69: "*Field reconnaissance is not carried out for this slope due to outbreak of the*
95   *COVID-19 pandemic. Instead, we examined the slope via Google Earth images. Fissure cracks is clearly visible on uppermost*
        part of the slope, and there are widespread cracks on the lower part of the slope. Evidenced by very high spatial resolution
        Google Earth images, the landslide in this work is a translational type (Highland and Bobrowsky 2013)."

        To echo on the landslide type, we called again on this topic in the discussion part (lines 219-224): "*... Because image*
        correlation methods use sliding windows to detect similar patterns between the base and target images, precursors with
100   *horizontal rather than vertical ground movements can be detected. Landslides that have intact moving surfaces can be*
        detectable by image correlation methods. For translational and rotational landslides, there are more horizontal than vertical

ground movements, which are ideal landslide types to use image correlation methods, whereas precursors of avalanches, rock falls may be difficult to detect due to limited horizontal ground movement (Highland and Bobrowsky 2013)."

105 3. On a minor note, there are two typos I have noticed.
         In section 2.2, you write "two twine satellites". Please change twine into twin.

         Similarly, in section 2.3, you write different illuminations, et al. (Stmpf et al. 2016). Please remove et al before the parentheses and correct the surname of the first author which should be Stumpf.

110 **Response**: Typos in these and other places were checked and corrected carefully.

~~Deriving slope movements~~Detecting precursors for an imminent landslide along the Jinsha River

Wentao Yang[1], Lianyou Liu[2,3,4], Peijun Shi[2,3,4]

[1]Three-gorges Reservoir Area (Chongqing) Forest Ecosystem Research Station, School of Soil and Water Conservation, Beijing Forestry University, Beijing, 100083, China
[2]Academy of Disaster Reduction and Emergency Management, Ministry of Emergency Management & Ministry of Education, Beijing Normal University, Beijing, 100875, China
[3]MOE, Key Laboratory of Environmental Change and Natural Disaster, Beijing Normal University, Beijing, 100875, China
[4]State Key Laboratory of Earth Surface Processes and Resource Ecology, Beijing Normal University, Beijing, 100875, China

Correspondence to: Lianyou Liu (lyliu@bnu.edu.cn) and Peijun Shi (spj@bnu.edu.cn)

Abstract. Landslides are major hazards that may pose serious threats to mountain communities. Even landslides in remote mountains could have non-negligible impacts on populous regions by blocking large rivers and forming ~~megafloods.~~dam-breached mega floods. Usually, there are slope deformations before major landslides occur, and detecting precursors such as slope movement before major landslides ~~occur~~is important for preventing possible disasters. In this work, we applied multi-temporal optical remote sensing images (Landsat 7 and Sentinel-2) and an image correlation method to detect sub-pixel slope deformations of a slope. ~~Near~~ near the Mindu town in the Tibet Autonomous Region~~, this~~. This slope is ~~also~~located ~~along~~on the right bank of the Jinsha River, ~80km downstream the famous Baige landslide. We used a DEM derived aspect to restrain background noises in image correlation results. We found the slope remained stable from November 2015 to November 2018 and moved significantly ~~from~~since November 2018~~ to November 2019~~. We used more data to analyse slope movement in 2019 and found retrogressive slope movements with increasingly large deformations near the river bank. We also analysed spatial-temporal patterns of the slope deformation from October 2018 to February 2020 and found seasonal variations in slope deformations. Only the foot of the slope~~foot~~ moved in dry seasons, whereas the entire slope activated in rainy seasons. Until 24 August 2019, the size of the slope with displacements larger than 3 m is similar to that of the Baige landslide. However, the river width at the foot of this slope is much narrower than the river width at the foot of the Baige landslide. We speculate it may continue to slide down and ~~dam~~threaten the Jinsha River. Further modelling works should be done to check if the imminent landslide could dam the Jinsha River and measures be taken to mitigate possible dammed breach flood disasters. This work illustrates the potential of using optical remote sensing to monitor slope deformations over ~~large~~remote mountain regions.

1 Introduction

Landslides are major natural hazards in mountain regions and have been causing widespread disasters every year around the globe (Petley 2012; Zhang et al. 2020). Major landslides in remote mountain regions may pose serious threats to downstream communities by choking channels to increase the risks of landslide-dammed lake outburst floods (Fan et al. 2020;

Liu et al. 2019). For example, a hillslope near the Baige village had two landslides, damming the Jinsha River twice in 2018.

145 The outburst floods caused widespread damage along its route and affected as far as Yunnan Province, > 500km from the landslides (Fan et al. 2019). In 2000, a super-large landslide dammed the Yigong River in Tibet and ~~two months later~~ the outburst flood ~~two months later~~ caused widespread damages, including 5 main bridges, highways and communication cables in downstream areas (Shang et al. ~~2013~~2003). The breach of the 1786 landslide-dammed lake in the Dadu river consumed >100,000 lives along its route (Dai et al. 2005). Similar cases could occur in many mountain regions in the world and detecting

150 precursors (such as slope movement) before major landslides is crucial for preventing such disasters (Intrieri et al. 2018; Carlà et al. 2019).

Remote sensing techniques have been an efficient way to monitor slope movement over large mountain regions (Du et al. 2020; Handwerger et al. 2019). Optical passive and ~~microwave active~~ radar remote sensing are most frequently used ~~tools~~data to detect slope displacements. There are two kinds of mainstream methods to derive slope movement. SAR

155 interferometry processing use the difference in phase images to derive subtle slope movement of a few millimetres (Intrieri et al. 2018; Samsonov et al. 2020). However, large ground displacements (e.g., a few metres), dense vegetation or long time intervals could lead to incoherence in phase images in this ~~types~~type of methods (Wasowski and Bovenga 2014). Image correlation methods (also referred as the pixel offset tracking used in SAR intensity images) is another type of methods that use SAR amplitude or optical images to ~~cross-correlating~~correlate image patches to measure slope movement, which can derive

160 sub-pixel ground displacements from 1/10 ~ 1/30 of a pixel (Li et al. 2020). The later type ~~of methods are~~is good at detecting larger slope movements that are visible on images (Bradley et al. 2019; Lacroix et al. 2020). In recent years, image correlation methods have been proposed and widely used to detect sub-pixel slope displacements in optical images (Bontemps et al. 2018; Lacroix et al. 2018, 2019~~; Lacroix et al. 2018~~; Yang et al. 2020).

In this work, using sub-pixel optical image correlation methods we report a landslide along the Jinsha River. Different

165 from previous retrospective studies, the landslide in this work did not collapse yet. ~~We speculate that~~We used multi-temporal Sentinel-2 images and found the slope is unstable and could pose a threat to downstream areas by blocking the Jinsha River~~. To test this hypothesis, we used multi-temporal Sentinel-2 images to detect possible slope displacements. We first used two Sentinel-2 images to find the relatively stable period before the flood caused by the upstream Baige landslide (October and November 2018). Then, we further analysed the movement of the slope after the flood from the Baige landslide in 2019~~.

170 **2 Methods**

2.1 Study Area

The reported slope is ~80 km downstream the Baige landslide (Fan et al. 2019) along the Jinsha River near the Mindu town, Tibet Autonomous Region, bordering Sichuan Province (Figure 1a). The slope is located on the right bank of the Jinsha River. Similar to the Baige landslide, the geomorphology of this section of the Jinsha River is at the bottom of V-shaped valley.

175 The elevation of the study area ranges from 2660m at the valley bottom to >4500m on the mountain ridge. This rough

topography indicates strong fluvial incision against the rapid uplift of the Tibetan Plateau. We estimated the mean annual precipitation (MAP) by using the GPM v6 monthly precipitation (from 2001 to 2019) and found the MAP of this area is ~665mm. The region is controlled by monsoon climate with >90% of the rain occurring from May to October. In addition, this

This area is tectonically active and active faults run through this slope from north to south. To the west of the faults are Upper Paleozoic strata, and to the east are Mesoproterozoic metamorphic rocks. Cracks and fissures on the slope is visible from the 15 m resolution pan-sharpened false colour Landsat 7 image acquired in 2001 (Figure 1b). These cracks and fissures may be relics of historic earthquakes or precipitations. This part of the slope has a percent slope of 45% and an aspect of the southeast, with azimuth between 112.5 °and 157.5 °(Figure 1c). ThisThe slope is mainly covered by grass and sparse shrubs and less affected by anthropogenic activities. Field reconnaissance is not carried out for this slope due to outbreak of the COVID-19 pandemic. Instead, we examined the slope via Google Earth images. Fissure cracks is clearly visible on uppermost part of the slope, and there are widespread cracks on the lower part of the slope. Evidenced by very high spatial resolution Google Earth images, the landslide in this work is a translational type (Highland and Bobrowsky 2013).

In this work, **2.2 The COSI-Corr method**

We mainly relied on Sentinel-2 optical images to derive slope movement. The European Space Agency's Sentienl-2 mission has two twinetwin satellites in orbit, with a revisit time of less than 5 days. The Sentinel-2 optical imagery has 12 optical bands with wavelength ranging from 440nm to 2200nm. (Gascon et al. 2017). There are 4 bands with a spatial resolution of 10m: blue, green, red and near infrared bands. To derive slope movement, we used the red band because its wavelength is longer than other visible bands and is less influenced by the atmosphere. Compared to the near infrared, this band is less sensitive to vegetation and is more reliable to measure slope deformation (Yang et al. 2019). We used the Level-1C product, which is already orthorectified before distribution (Gascon et al. 2017).

2.2 The COSI-Corr method

This work used the COSI-Corr method, a correlation method for optical images, to detect slope displacements (Leprince et al. 2007). To derive slope movement, two imageimages in a roll should be used to form an image pair, including the base image and the target image. The base image is an earlier image, based on which image correlation algorithm (here we use the COSI-Corr) is implemented to detect slope displacements in the target image (Leprince, et al. 2007). For detailed parameters to use the COSI-Corr method, please refer to Yang, et al. (2019b2020).

In this work, twowe used three steps were taken to detect slope displacements. First for the studied Mindu slope. For the first step, we used two image pairs (#1-#2) to detect slope movementfind the stable and moving periods before and after November 2018. For thisFor the second step, we used 19 images in the stable period to estimate cumulative slope displacements in 5 images in the moving period (image pair #3-#97). For the third step, we used another nine images to derive displacements for every two adjacent images (image pair #98-#105).

2.2.1 Deriving slope displacements

In the first step, we used three Sentinel-2 images on 13 November 2015, 12 November 2018 and 12 November 2019 to compose two image pairs~~.~~ (#1 and #2). The first image pair (#1) is composed of a Sentinel-2 image on 13 November 2015 and a Sentinel-2 image on 12 November 2018. Sentinel-2 images of the second pair (#2) are acquired on 12 November 2018 and on 12 November 2019. ~~Both image pairs are composed of Sentinel-2 images of similar dates of different years to minimize the influence of solar elevation angles (Yang et al. 2020).~~

~~We~~By using the first two image pairs, we found the slope was stable from 13 November 2015 to 12 November 2018 and moved significantly from 12 November 2018 to 12 November 2019. Therefore, in the second step, we further used two image groups, a base image group and a target image group, to detect cumulative slope displacements ~~and estimate uncertainties~~ (Table 1). For the base image group, there are 19 images~~, all of which are acquired~~ in early 2018. These selected 19 base images are clear images without clouds in ~~2018. Although Sentinel-2 images have very short revisit time, most images are contaminated by clouds on the Mindu slope before September 2018.~~the stable period. For the target image group, we selected five images in 2019 (13 April, 17 July, 24 August, 5 October and 12 November) to detect ~~slope displacements. For each target image in 2019, average slope displacements and uncertainties are estimated from all 19 base images by forming 19 image pairs in the COSI-Corr method, separately.~~ cumulative displacements. In all, there are 19×5 image pairs ~~are~~(#3-#97) calculated in the second step. In the third step, we use nine images from 28 September 2018 to 7 February 2020 (Table 2) to form another eight image pairs (#98-#105) to derive slope displacements.

2.~~3~~2.2 Error Assessment and postprocessing

~~There are some uncertainties in using image correlation methods, which may be caused by different viewing angles of images, different illuminations, et al. (Stmpf et al. 2016). The first two image pairs we mentioned above are composed by two images of very similar acquire dates of different years. Images of similar dates have similar zenith/elevation angles, which could minimize the influence of mountain shadows (Yang et al. 2020). In addition, misalignment~~Misalignments between images can be estimated by selecting a stable zone (Bontemps et al. 2018; Lacroix et al. 2018; Yang et al. 2019). ~~Mean displacements estimated within the stable zone will be used to correct image shifts. The stable zone in~~In this work~~,~~, the stable zone was selected on the upper part of the landslide (red rectangular in Fig 1b and 1c). Mean displacements estimated within the stable zone were used to correct image shifts. Standard deviations of the displacements within the stable zone represents uncertainties, indicating the quality of the derived results for a given image pair. We select this area because this stable zone is on the same slope as the landslide, which can minimize the influence of illumination and errors during orthorectification.

~~To derive spatial-temporal slope deformation patterns~~In this work, we ~~used nine images from 28 September 2018 to 7 February 2020 (Table 2) to form eight image pairs (periods) to derive~~cross-validated measured slope displacements ~~for five target images~~ in ~~different periods. All~~2019 in the second step. Uncertainties of the slope displacements ~~were corrected by using~~for a given target image are estimated from all 19 base images in the stable ~~zone (the rectangular with red boundary in~~

8

~~Figure 1b&1c).~~periods. Standard deviations of these 19 measurements were used to indicate their reliability. We further ~~used~~
~~the SRTM DEM derived aspect to~~ filter out ~~derived slope movement~~displacements with moving directions that does not agree
with the ~~aspect.~~SRTM DEM derived aspects. If there are 15 ° deviations between the derived slope movement and the aspect,
the derived slope movement is defined as ~~not valid~~invalid and will not be used for further analysis. ~~This is reasonable for
translational landslides as the mass moves downhill driven by gravity. Evidenced by optical images, the landslide in this work
is a translational type and could be dealt with in this way (Highland and Bobrowsky 2013).~~

3 Results

3.1 Detected stable and unstable periods

In Table 3, ~~The~~the EW-mean and NS-mean indicate the east-west (EW) and north-south (NS) shifts of images in both
image pairs calculated from the stable zone. The EW-std and NS-std ~~measures image distortions~~are standard deviations of
displacements in the stable zone to indicate image distortions. Low EW-std and NS-std values indicates good performances
during image orthorectifications. The derived EW-mean and NS-mean were ~~then~~used to correct ~~misalignment~~misalignments
in ~~images~~image pairs.

~~For~~The base and target images for image pair #1~~, the base image is acquired~~ are on 13 November 2015 and ~~the second
image is acquired~~12 November 2018, respectively. The base and target images for image pair #2 are on 12 November 2018
and 12 November 2019, respectively. The slope remains stable in the first image pair, whereas detectable slope displacements
can be found in the second image pair (Figure 2). The ~~duration~~durations of ~~the first~~ image pair ~~spans~~#1 and pair #2 span 3
years and ~~the second image pair lasts~~ one year~~.~~, respectively. In Figure 2a, we can see that the slope displacement from ~~13
November~~ 2015 to ~~12 November~~ 2018 was less than 2 m, whereas there was ~~more than~~ ≥6 m slope displacement from ~~12
November~~ 2018 to ~~12 November~~ 2019 (Figure 2b). In image pair #2, larger displacements were observed near the Jinsha River
and smaller displacements were farther away from the river. This increasing displacement magnitude ~~may~~indicate the slope
may start to move ~~since~~from its toe.

3.2 ~~Slope~~ Cumulative slope displacements in 2019

As in Figure 2, we can see that ~~the~~this slope ~~remains~~remained stable from November 2015 to November 2018 and ~~is
moving~~moved after November 2018. To derive time series of the Mindu slope displacements after November 2018, we used
19 base images in the stable period and 5 target images in 2019. All 19 base images are from early 2018, during which the
slope was stable. Five selected target images are acquired on 13 April 2019, 17 July 2019, 24 August 2019, 5 October 2019
and 12 November 2019. For each target image in 2019, we calculated slope movement by using all base images. Therefore,
there are 19 estimated slope displacements for each target image. We calculated the means and standard deviations of slope
displacements for ~~each target image representing slope movement from early 2018 and six periods in 2019~~all target images
(Figure 3).

270   From Figure 3, we can see that the mean displacements are a magnitude larger than standard deviations, which indicate that the displacements derived between each target image and their base images agree with each other quite well. Minor slope displacements were detected until April 2019 (maximum 3~4m), whereas larger slope displacements can be observed in the later four target images (>5 m). All displacements in five target images show a similar pattern with results in image pair 2 (Figure 2b), demonstrated by larger displacements near the river and less movement further from the river.

275   ~~However, the third target image (24 August 2019) has more displacement of large values than other target images. As seen from Figure 3, it is quite possible that the slope moved significantly during 2019.~~

We further selected six points on the slope to analyse time series of the slope displacements in 2019 (Figure 4). For most target images in the first five points (p1-p5), most base images could derive >10 valid displacements (2-D columns). For all six points, accumulated displacements show similar growing trends from April 2019 to November 2019. Maximum

280   displacements in all six points occurred on 24 August 2019. These unreasonably large values may be caused by difference of solar elevation/zenith angles in target images. For example, compared to the August image there are more mountain shadows in the November images in northern hemisphere. Despite abnormal displacements in August 2019, we can still see that displacements from July to November 2019 are still larger than displacements in April 2019. Therefore, from time series of these six points, we can see that major slope displacements occurred from April to August 2019.

285   **3.3 Slope displacements in eight selected periods after November 2018**

To analyse spatial deformation patterns in different periods, we selected 9 Sentinel-2 images forming eight image pairs (image pairs #98-#105 in Table 2, corresponding to eight periods in ~2 months). The first two image pairs (Figure 5a-b, #98 and #99) shows that the middle and lower parts of the slope deformed significantly and 4-6 meters of displacement occurred at multiple locations. The study area has a monsoonal climate with most precipitation occurs from May to September

290   (Figure 6). There are seasonal differences in deformation of this landslide. In dry seasons of winter and spring, deformation occurs at the foot of the slope near the Jinsha River and deformation rate is generally less than 1 m/month (from January to May, Figure 5c&d and periods 3-4 in Figure 6~~).~~. image pairs #100-#101). In rainy seasons of summer and autumn, deformation affects the entire slope with some parts at a rate of more than 3 meters/month (from May to September, Figure 5e&f and periods 5-6 in Figure 6, image pairs #102-#103).

295   **4 Discussion**

4.1 Possible impacts of this imminent landslide

Major landslides in mountains may dam river channels forming transient lakes, the breach of which can result in catastrophic floods to downstream communities (Dai et al. 2005; Fan et al. 2019; Liu et al. 2019). In this work, we examined a hillslope near the Mindu town along the Jinsha River. We found the slope had significant movement from November 2018

300   to November 2019. Despite the area of the detected moving slope (715,577 m^2 for displacements larger than 3 m) is similar

10

with the area of the Biage landslide (830,624 m^2), the width of the Jinsha River channel below the Mindu slope (~ 50) is half that of the Baige (>100 m, in Figure 7). Considering the similar morphology of both river sections, the collapse of the Mindu slope ~~may~~could pose a threat to downstream communities by blocking the Jinsha River. We call for further frequent monitoring of the hillslope in combination with other tools, such as InSAR (Intrieri et al. 2018; Samsonov et al. 2020).

305 ~~There are a few strategies to suppress background noises in derived results, including selecting results with high signal/noise ratios (Lacroix et al. 2018; Yang et al. 2020), integrating redundant information in time series of images (Bontemps et al. 2018). This work introduced a new method to use slope aspect to filter out slope movement that is different from the aspect. This procedure could eliminate false slope movements and reserves true slope movement of the Mindu landslide.~~

4.2 Comparison of image matching and InSAR methods

310 In this work, we used the COSI-Corr method to derive slope displacements for the Mindu slope along the Jinsha River. The principle of this method is to use a sliding window to find pattern matches to derive displacements in image pairs (Leprince et al. 2007). Compared to the InSAR methods, this method is easier to understand and implement. In addition, image correlation methods favour larger displacements than InSAR methods. Limited by the wavelength of SAR image, InSAR methods are versed in monitoring ground deformation of millimetre to centimetre scale (Intrieri et al. 2018), whereas the capability of 315 image correlation methods depends on spatial resolution of images. In general, image correlation methods are more reliable for deriving large ground displacements of metre scale (Bradley et al. 2019; Lacroix et al. 2020). In this work, it might be quite challenging for InSAR methods to detect such large displacements.

Long temporal intervals of a few months could lead to incoherence in SAR images (Li et al. 2019), whereas images (taken on the same season) with long temporal intervals of a few years can be used to derive reliable displacements given 320 stable land cover (Yang 2020). Both type of methods can be affected by the atmosphere. Clear optical images without clouds should be used in image correlation methods. Although SAR images could penetrate thin clouds, atmosphere could cause phase delay and lead to uncertainties in derived results (Li et al. 2019).

Both methods work well on bare land without vegetation, though dense vegetation could seriously affect InSAR methods (Intrieri et al. 2018). On the contrary, image correlation methods are less affected by vegetation cover as long as both 325 images in a pair are from the same season (Yang 2020). As image correlation methods use pattern matches within an image pair, we speculate that vegetation density may not be a major challenge on derived results. The Sentinel-2 images used in this work have four 10-metre resolution optical bands (Gascon et al. 2017). In theory, any of these four bands may be used to derive slope displacements. But, an ideal band should not be sensitive to ground cover change unrelated with ground displacements, which could minimize background noises. In general, optical bands with shorter wavelength is more prone to 330 be affected by moisture in the atmosphere. Considering that near infrared band is very sensitive to vegetation, we used the red band in this work.

Both InSAR and image correlation methods can be impacted by complex terrains in mountain regions. Layover and shadow areas in SAR images should not be used in InSAR methods (Li et al. 2019). Similarly, shadows in optical images also

11

influence derived results (Yang et al. 2020). To derive reliable results, optical images acquired during larger solar angles should be prioritized to minimize the influence of mountain shadows. Fortunately, there are algorithms developed to restore information in mountain shadows in optical images (Shahtahmassebi et al. 2013), which may promote the efficacy of optical image correlation methods.

4.3 Measures taken to reduce uncertainties

Many other factors canmay also influence the accuracy of slope deformation derivations by usingfrom image correlation methods, which includes errors during image orthorectification errors, different viewing angles of imagesduring image acquisition, different illuminations in images, et al. (StmpfStumpf et al. 2016; Yang et al. 2020). This work used Sentinel-2 L1C product, which is already orthorectified before distribution (Gascon et al. 2017). To correct for possible mis-registration between the base and mastertarget images, we used a stable zone to calculate and correct image shifts. To reduce errors caused by different illuminations and viewing angles of images during acquisition, all images used for the first two Sentinel-2 image pairs are from similar dates of different years. To derive cumulative displacements, we used 19 base images in early 2018 to detect slope displacements in five target images in 2019.

The first two image pairs (#1 and #2) we mentioned above are composed of images of very similar acquire dates in different years. Images of similar dates have similar zenith/elevation angles, which could minimize the influence of mountain shadows (Yang et al. 2020). To assess and reduce uncertainties in the second step, we first identified a stable period. Then, we used 19 base images in this stable period to derive cumulative displacements for a given target image in the moving period. The mean displacements from these 19 image pairs are expected to be more reliable than results from a single image pair. In addition, these 19 measurements can cross-validate each other and be used to estimate uncertainties by standard deviations (Figure 3 and Figure 4).

There are a few strategies to suppress background noises in derived results, including selecting results with high signal/noise ratios (Lacroix et al. 2018; Yang et al. 2020), integrating redundant information in time series of images (Bontemps et al. 2018). This work introduced a simple and efficient way by using slope aspect to filter out slope movement that is different from the aspect. This is reasonable for this translational landslide as the mass moves downhill driven by gravity. This procedure could eliminate false slope movements and reserves true slope movement of the Mindu landslide. By integrating topographic information, this new procedure is expected to work well for ground movement in other regions that is consistent with slope configurations.

4.4 Potential applications of the method in landslide monitoring

As we used orthorectified images, slope displacements derived in this work are horizontal movements. To derive ground movement along the slope, we need to consider local slope configurations. Because image correlation methods use sliding windows to detect similar patterns between the base and target images, precursors with horizontal rather than vertical ground movements can be detected. Landslides that have intact moving surfaces can be detectable by image correlation

12

methods. For translational and rotational landslides, there are more horizontal than vertical ground movements, which are ideal landslide types to use image correlation methods, whereas precursors of avalanches, rock falls may be difficult to detect due to limited horizontal ground movement (Highland and Bobrowsky 2013).

In addition, the smallest displacements that can be detected depends on the spatial resolution of optical images (Li et al. 2020, Stumpf et al. 2016). Although image correlation methods can detect sub-pixel ground movement, it is very challenging to detect moving surfaces that cover an area of a few pixels, as smaller window sizes could result in more background noises (Yang et al. 2020).

5 Conclusions

In this work, by using the COSI-Corr method and multi-temporal Sentinel-2 images, we found precursors of a major landslide along the Jinsha River in southwest China. Fissures on the slope probably existed before 2001 but the slope remained stable between November 2015 and November 2018. From November 2018 to August 2019, we detected significant slope displacements. The size of the activated part on the Mindu slope is similar to that of the 2018 Baige landslide, whereas the river width under the Mindu slope is half width of the Baige section. If this landslide continues to slide down and fails completely, it may block the Jinsha River leading to similar consequences as the Baige landslide.

By using image correlation technique, we can track sub-pixel slope movement in optical remote sensing images. We also adopted an aspect constraint to ~~automatically~~ pick out downslope movement and significantly depressed ~~much of the~~ background ~~noise. We applied these techniques on multi-temporal Sentinel-2 images to detect slope movement near the Mindu town along the Jinsha River. We found the Mindu landslide probably existed before 2001 and the slope remains relatively stable between November 2015 and November 2018. Significant slope displacements were observed from November 2018 to August 2019.~~

~~We found the size of the Mindu slope that activated is similar to that of the Baige landslide, whereas the river width under the Mindu slope is half of the Baige section. If the Mindu landslide continues to slide down and occur, it may block the Jinsha River leading to similar social economic consequences as the 2018 Baige landslide~~noises. However, optical images, such as the Sentinel-2 images, can only detect slope movements up to a few metres. To ~~derive minor~~ continuously monitor this slope ~~displacements,~~, other data and methods (such as higher spatial resolution images or InSAR techniques) should be ~~implemented for this remote slope.~~used. We also call for ~~continuous~~intensive monitoring of this slope and modelling of ~~landslides caused river blocking and subsequent flooding~~the landslide's impacts.

Data availability. All Sentinel-2 images and the Landsat 8 image in this work were downloaded from the GEE. The SRTM DEM and its derivative were downloaded from the Geospatial Data Cloud website (http://www.gscloud.cn/sources).

Supplement. There is no related supplement for this paper.

Author contribution. LL and PS discovered the moving slope of this work. WY conducted analysis and drafted the manuscript.

References

Bontemps, N., Lacroix, P., and Doin, M.-P.: Inversion of deformation fields time-series from optical images, and application to the long term kinematics of slow-moving landslides in Peru. Remote Sens. Environ., 210, 144-158, https://doi.org/10.1016/j.rse.2018.02.023, 2018.

Bradley, K., Mallick, R., Andikagumi, H., Hubbard, J., Meilianda, E., Switzer, A., Du, N., Brocard, G., Alfian, D., Benazir, B., Feng, G., Yun, S.-H., Majewski, J., Wei, S., and Hill, E.M.: Earthquake-triggered 2018 Palu Valley landslides enabled by wet rice cultivation. Nat. Geosci., 12, 935-939, https://doi.org/10.1038/s41561-019-0444-1, 2019.

Carlà, T., Intrieri, E., Raspini, F., Bardi, F., Farina, P., Ferretti, A., Colombo, D., Novali, F., and Casagli, N.: Perspectives on the prediction of catastrophic slope failures from satellite InSAR. Scientific Report, 9, 14137, https://doi.org/10.1038/s41598-019-50792-y, 2019.

Dai, F., Lee, C., Deng, J., and Tham, L.G.: The 1786 earthquake-triggered landslide dam and subsequent dam-break flood on the Dadu River, southwestern China. Geomorphology, 65, 205-221, https://doi.org/10.1016/j.geomorph.2004.08.011, 2005.

Du, J., Glade, T., Woldai, T., Chai, B., and Zeng, B.: Landslide susceptibility assessment based on an incomplete landslide inventory in the Jilong Valley, Tibet, Chinese Himalayas. Eng. Geol., 270, 105572, https://doi.org/10.1016/j.enggeo.2020.105572, 2020.

Fan, X., Dufresne, A., Subramanian, S.S., Strom, A., Hermanns, R., Stefanelli, C.T., Hewitt, K., Yunus, A.P., Dunning, S., Capra, L., Geertsema, M., Miller, B., Casagli, N., Jansen, J.D., and Xu, Q.: The formation and impact of landslide dams – State of the art. Earth-Science Reviews, 203, 103116, https://doi.org/10.1016/j.earscirev.2020.103116, 2020.

Fan, X., Xu, Q., Alonso-Rodriguez, A., Subramanian, S.S., Li, W., Zheng, G., Dong, X., and Huang, R.: Successive landsliding and damming of the Jinsha River in eastern Tibet, China: prime investigation, early warning, and emergency response. Landslides, 16, 1003-1020, https://doi.org/10.1007/s10346-019-01159-x, 2019.

Gascon, F., Bouzinac, C., Thépaut, O., Jung, M., Francesconi, B., Louis, J., Lonjou, V., Lafrance, B., Massera, S., Gaudel-Vacaresse, A., Languille, F., Alhammoud, B., Viallefont, F., Pflug, B., Bieniarz, J., Clerc, S., Pessiot, L., Trémas, T., Cadau, E., De Bonis, R., Isola, C., Martimort, P., and Fernandez, V.: Copernicus Sentinel-2A Calibration and Products Validation Status. Remote Sens., 9(6), 584, https://doi.org/10.3390/rs9060584, 2017.

Handwerger, A.L., Fielding, E.J., Huang, M., Bennett, G.L., Liang, C., Schulz, W.H.: Widespread Initiation, Reactivation, and Acceleration of Landslides in the Northern California Coast Ranges due to Extreme Rainfall. J. Geophys Res-Earth, 124, 1782-1797, https://doi.org/10.1029/2019JF005035, 2019

Highland, L. and Bobrowsky, P.: The Landslide Handbook—a Guide to Understanding Landslides: A Landmark Publication for Landslide Education and Preparedness. Springer Berlin Heidelberg. 2013.

Intrieri, E., Raspini, F., Fumagalli, A., Lu, P., Del Conte, S., Farina, P., Allievi, J., Ferretti, A., and Casagli, N.: The Maoxian landslide as seen from space: detecting precursors of failure with Sentinel-1 data. Landslides, 15, 123-133, https://doi.org/10.1007/s10346-017-0915-7, 2018.

Lacroix, P., Araujo, G., Hollingsworth, J., and Taipe, E.: Self-Entrainment Motion of a Slow-Moving Landslide Inferred From Landsat-8 Time Series. J. Geophys Res-Earth, 124, 1201-1216, https://doi.org/10.1029/2018jf004920, 2019.

Lacroix, P., ~~Berthier, E., and Maquerhua, E.T.: Earthquake-driven acceleration of slow-moving landslides in the Colca valley, Peru, detected from Pléiades images. Remote Sens. Environ., 165, 148-158, https://doi.org/10.1016/j.rse.2015.05.010, 2015.~~

~~Lacroix, P.,~~ Bièvre, G., Pathier, E., Kniess, U., and Jongmans, D.: Use of Sentinel-2 images for the detection of precursory motions before landslide failures. Remote Sens. Environ., 215, 507-516, https://doi.org/10.1016/j.rse.2018.03.042, 2018.

Lacroix, P., Dehecq, A., and Taipe, E.: Irrigation-triggered landslides in a Peruvian desert caused by modern intensive farming. Nat. Geosci., 13, 56-60, https://doi.org/10.1038/s41561-019-0500-x, 2020.

Leprince, S., Barbot, S., Ayoub, F., and Avouac, J.: Automatic and Precise Orthorectification, Coregistration, and Subpixel Correlation of Satellite Images, Application to Ground Deformation Measurements. IEEE T. Geosci. Remote, 45, 1529-1558, https://doi.org/10.1109/TGRS.2006.888937, 2007.

Li, M., Zhang, L., Ding, C., Li, W., Luo, H., Liao, M., and Xu, Q.: Retrieval of historical surface displacements of the Baige landslide from time-series SAR observations for retrospective analysis of the collapse event. Remote Sens. Environ., 240, 111695, https://doi.org/10.1016/j.rse.2020.111695, 2020.

Li, Z., Song, C., Yu, C., Xiao, R., Chen, L., Luo, H., Dai, K., Ge, D., Ding, Y., Zhang, Y., Zhang, Q.: Application of satellite radar remote sensing to landslide detection and monitoring: challenges and solutions. Geomatics and Information Science of Wuhan University, 44(7): 967-979, http://dx.doi.org/10.13203/j.whugis20190098, 2019.

Liu, W., Carling, P., Hu, K., Wang, H., Zhou, Z., Zhou, L., Liu, D., Lai, Z., and Zhang, X.: Outburst floods in China: A review. Earth-Science Reviews, 197, 102895, https://doi.org/10.1016/j.earscirev.2019.102895, 2019.

~~Luo, S., Jin, X. and Huang, D.: Long-term coupled effects of hydrological factors on kinematic responses of a reactivated landslide in the Three Gorges Reservoir. Eng. Geol., 261, 105271, https://doi.org/10.1016/j.enggeo.2019.105271, 2019.~~

Petley, D.: Global patterns of loss of life from landslides. Geology, 40, 927-930, https://doi.org/10.1130/G33217.1, 2012.

Samsonov, S., Dille, A., Dewitte, O., Kervyn, F., and d'Oreye, N.: Satellite interferometry for mapping surface deformation time series in one, two and three dimensions: A new method illustrated on a slow-moving landslide. Eng. Geol., 266, 105471, https://doi.org/10.1016/j.enggeo.2019.105471, 2020.

Shahtahmassebi, A., Yang, N., Wang, K., Moore, N., and Shen, Z.: Review of shadow detection and de-shadowing methods in remote sensing. Chin. Geogr. Sci. 23, 403–420, https://doi.org/10.1007/s11769-013-0613-x, 2013.

Shang, Y., Yang, Z., Li, L., Liu, D., Liao, Q., and Wang, Y.: A super-large landslide in Tibet in 2000: background, occurrence, disaster, and origin. Geomorphology, 54(3-4), 225-243, https://doi.org/10.1016/S0169-555X(02)00358-6, 2003.

465 Stumpf, A., Malet, J.P., Puissant, A., and Travelletti, J.: Monitoring of Earth Surface Motion and Geomorphologic Processes by Optical Image Correlation. Land Surface Remote Sensing, 147-190, https://doi.org/10.1016/B978-1-78548-105-5.50005-0, 2016.

Wasowski, J. and Bovenga, F.: Investigating landslides and unstable slopes with satellite Multi Temporal Interferometry: Current issues and future perspectives. Eng. Geol., 174, 103-138, https://doi.org/10.1016/j.enggeo.2014.03.003, 2014.

470 Yang, W., Wang, Y., Sun, S., Wang, Y., and Ma, C.: Using Sentinel-2 time series to detect slope movement before the Jinsha River landslide. Landslides, 16, 1313-1324, doi: 10.1007/s10346-019-01178-8, 2019.

Yang, W.: Selecting the best image pairs to measure slope deformation. Sensors, 20(17), 4721, https://doi.org/10.3390/s20174721, 2020.

Yang, W., Wang, Y., Wang, Y., Ma, C., and Ma, Y.: Retrospective deformation of the Baige landslide using optical remote

475 sensing images. Landslides, 17, 659-668, https://doi.org/10.1007/s10346-019-01311-7, 2020.

Zhang, S., Li, C., Zhang, L., Peng, M., Zhan, L., and Xu, Q.: Quantification of human vulnerability to earthquake-induced landslides using Bayesian network. Eng. Geol., 265, 105436, https://doi.org/10.1016/j.enggeo.2019.105436, 2020.

480
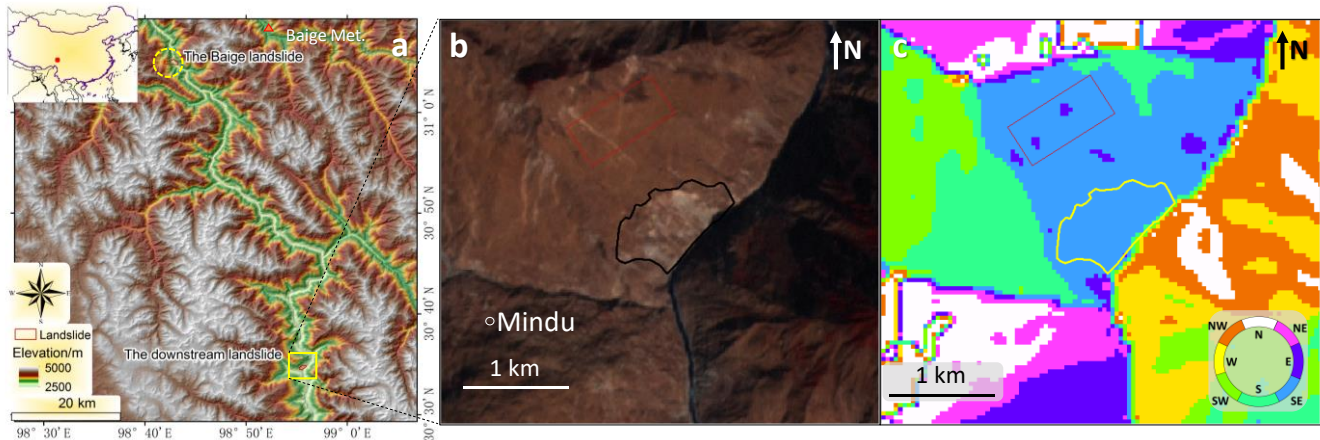
Figure 1: Topographic maps of the study area. (a) Geographic locations of the Baige landslide and the downstream landslide around the Mindu town, Tibet Autonomous Region. (b) A 15 m resolution pan-sharpened Landsat 7 false colour image on 18 February 2001 and (c) aspect of the study area around the Mindu landslide (The elevation data in a is a product of the NASA's Shuttle Radar

485 **Topography Mission (SRTM) and the aspect in c is a derivative of the DEM. The red polygons in b and c are the selected stable zone. Both the SRTM DEM in (a) and its derivative (c) are downloaded from the Geospatial Data Cloud website**
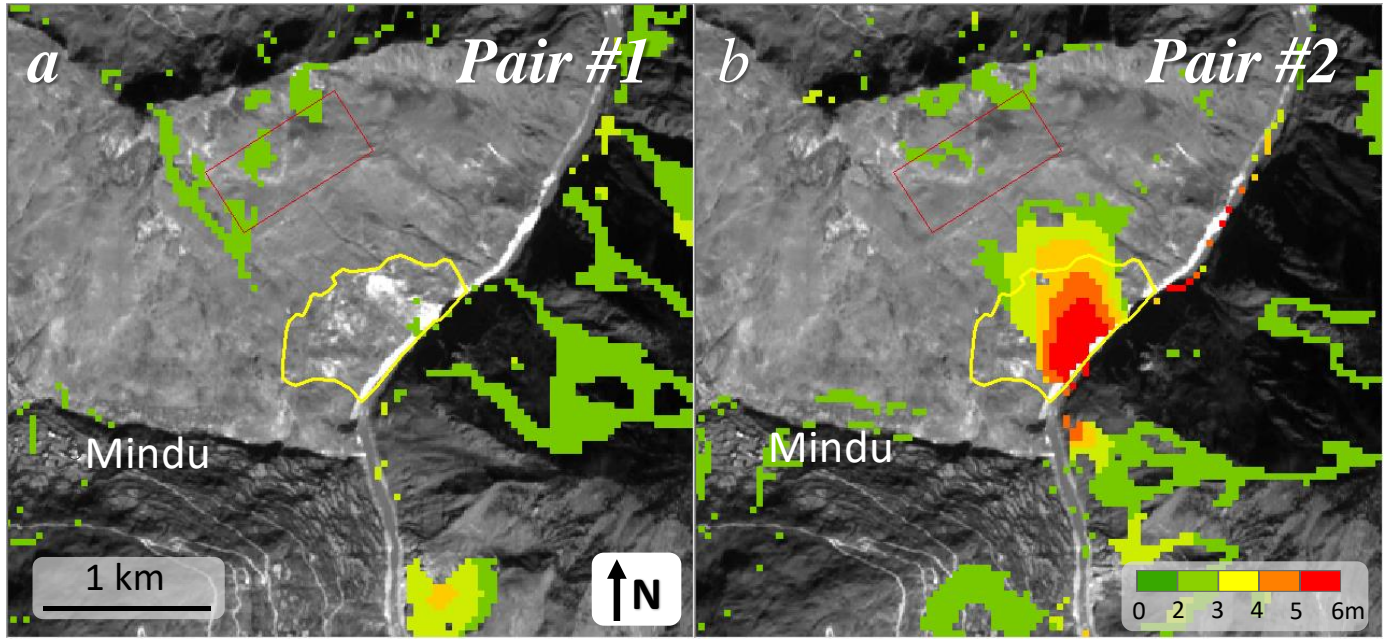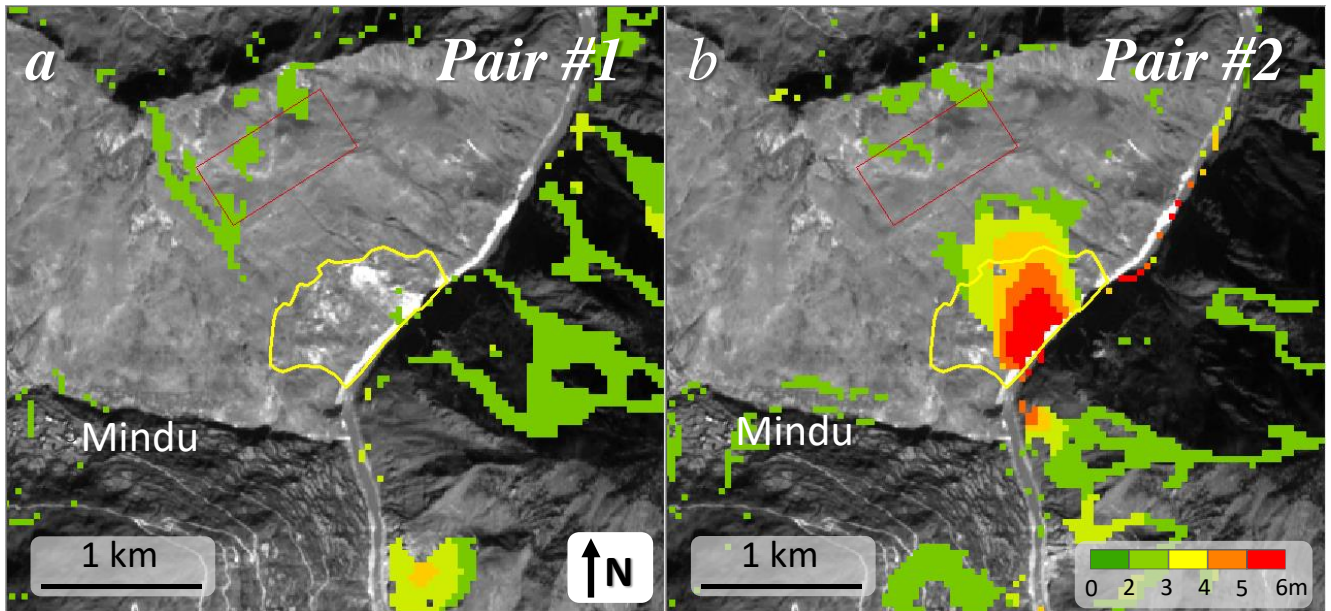
Figure 2: Detected slope displacements in image pairs #1 and #2 (Background Sentinel-2 images are acquired on 13 November 2015 and 12 November 2018, respectively. Both images were produced by the ESA's Sentinel-2 satellites and downloaded via the GEE).
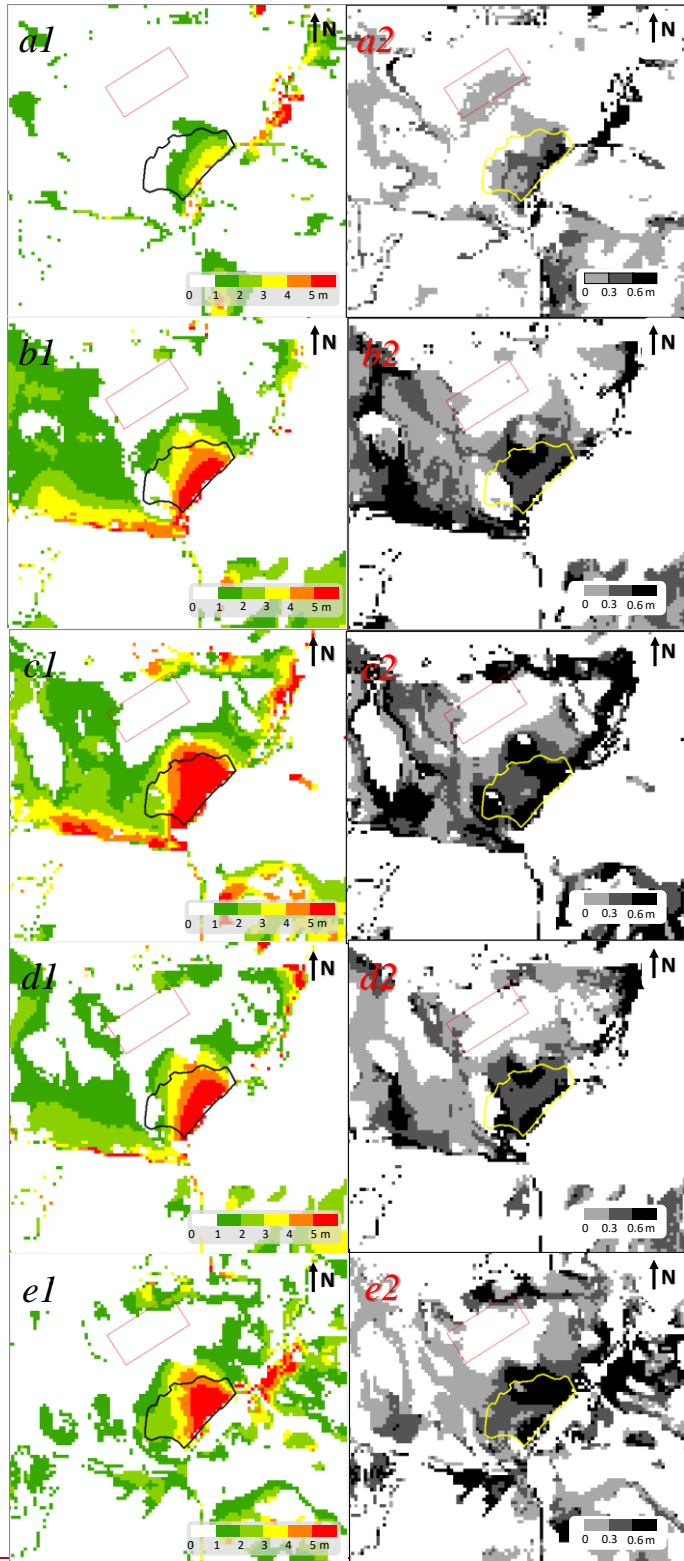
Figure 3: Means and standard deviations of derived slope displacements in nine targeted images (Tab. 2). Detected means and standard deviations of slope displacement on 13 Apr. 2019 (*a1-a2*), 17 Jul. 2019 (*b1-b2*), 24 Aug. 2019 (*c1-c2*), 5 Oct. 2019 (*d1-d2*), 12 Nov. 2019 (*e1-e2*), respectively.
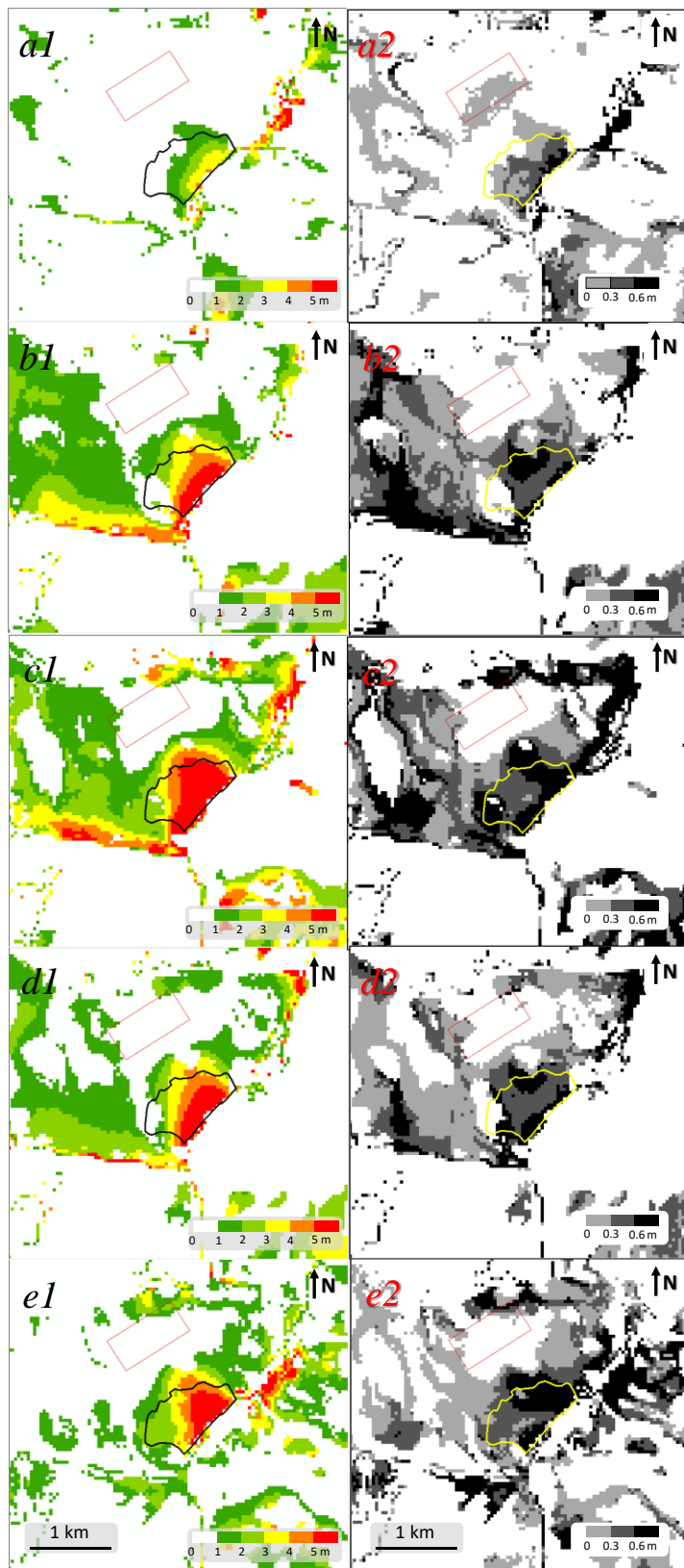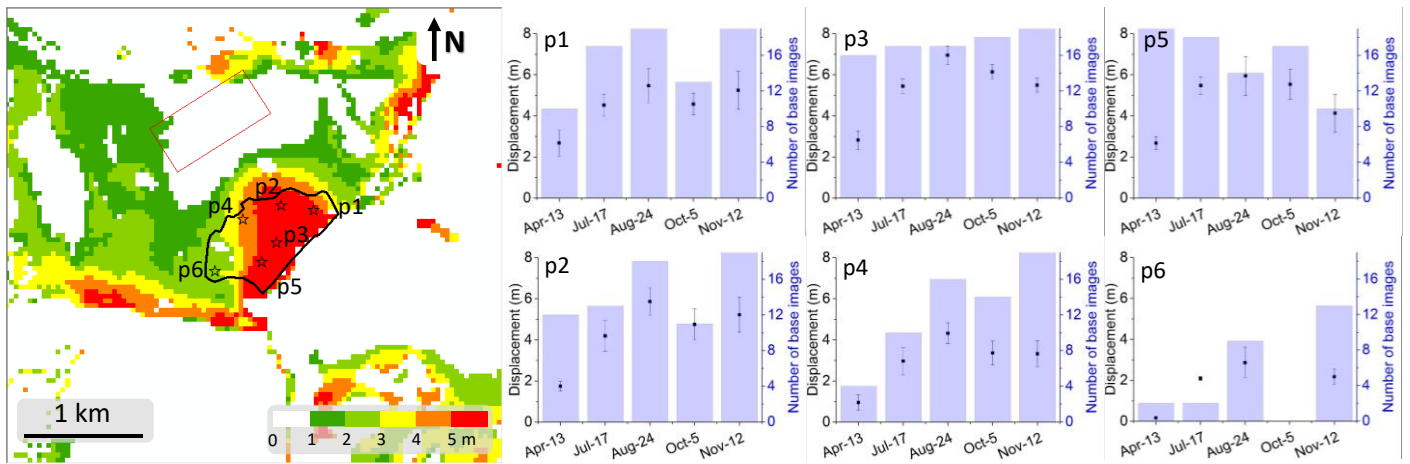
Figure 4: Time series of slope displacements for the six target images. Image to the left shows slope displacements shown above the Sentinel-2 image on 12 November 2019 and map colour is shown in minimum-maximum linear stretch type. Sub-panels p1-p6 show means (points), standard deviations (vertical bars) and valid numbers (histograms) of cumulative displacements between 19 base and 5 target images for the six selected points (stars) in the left image.
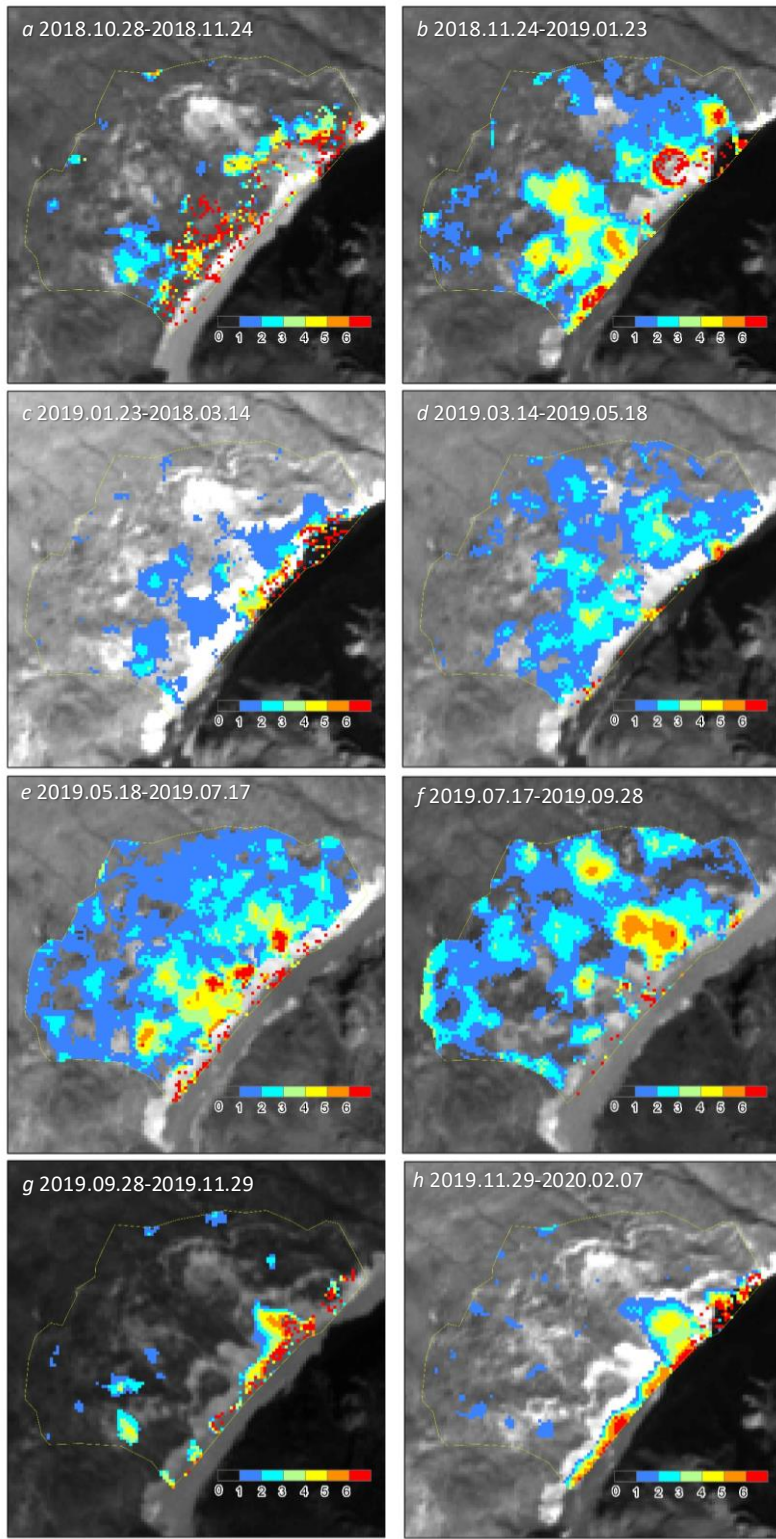
Figure 5: Slope displacements in different periods after the Baige floods (Background images are Sentinel-2 data produced by the ESA's Sentinel-2 satellites and downloaded via the GEE).

a 2018.10.28-2018.11.24

b 2018.11.24-2019.01.23

c 2019.01.23-2018.03.14

d 2019.03.14-2019.05.18

e 2019.05.18-2019.07.17

f 2019.07.17-2019.09.28

g 2019.09.28-2019.11.29

h 2019.11.29-2020.02.07

500 m
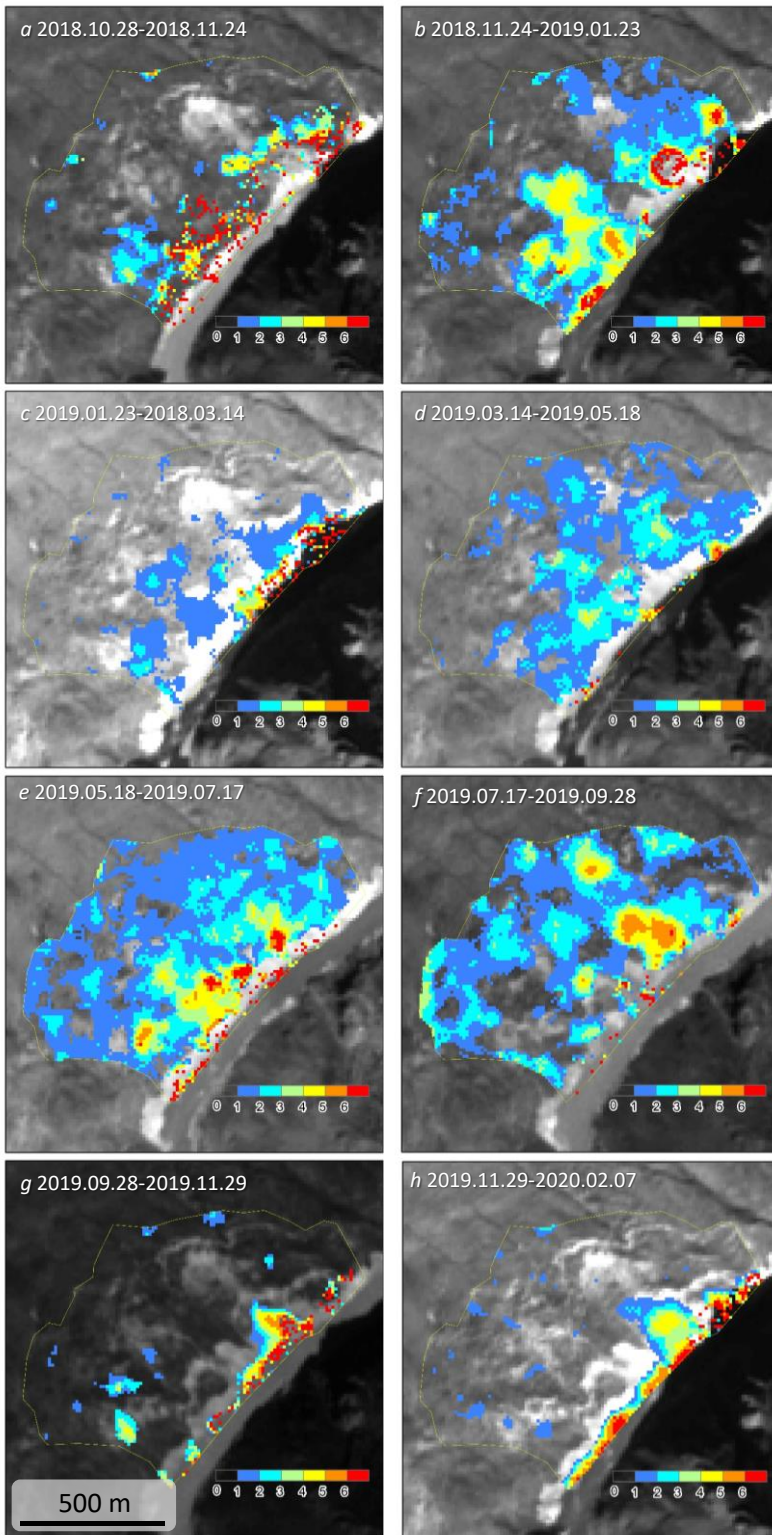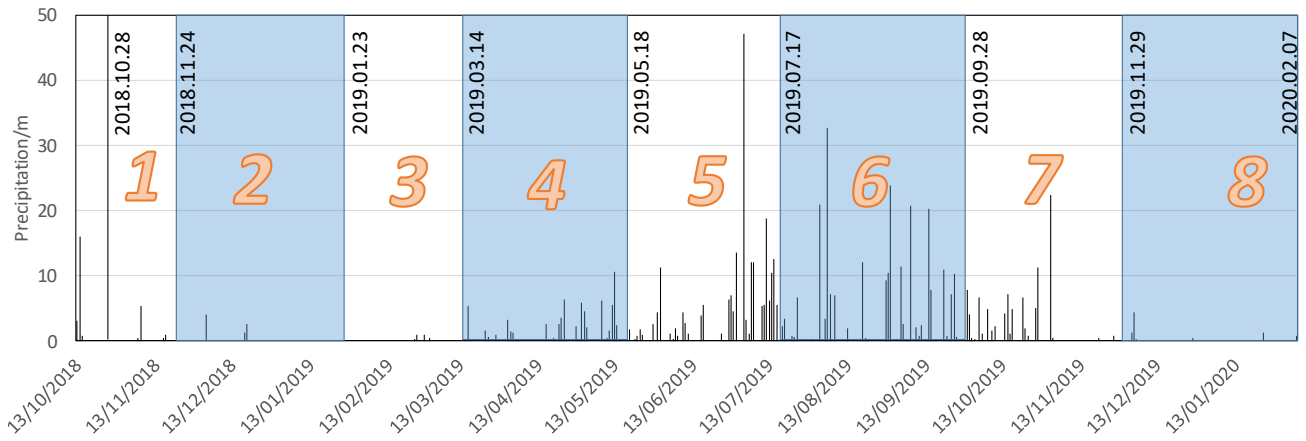
Figure 6: Daily precipitation of the Baiyu Meteorology station from October 2018 to February 2020.
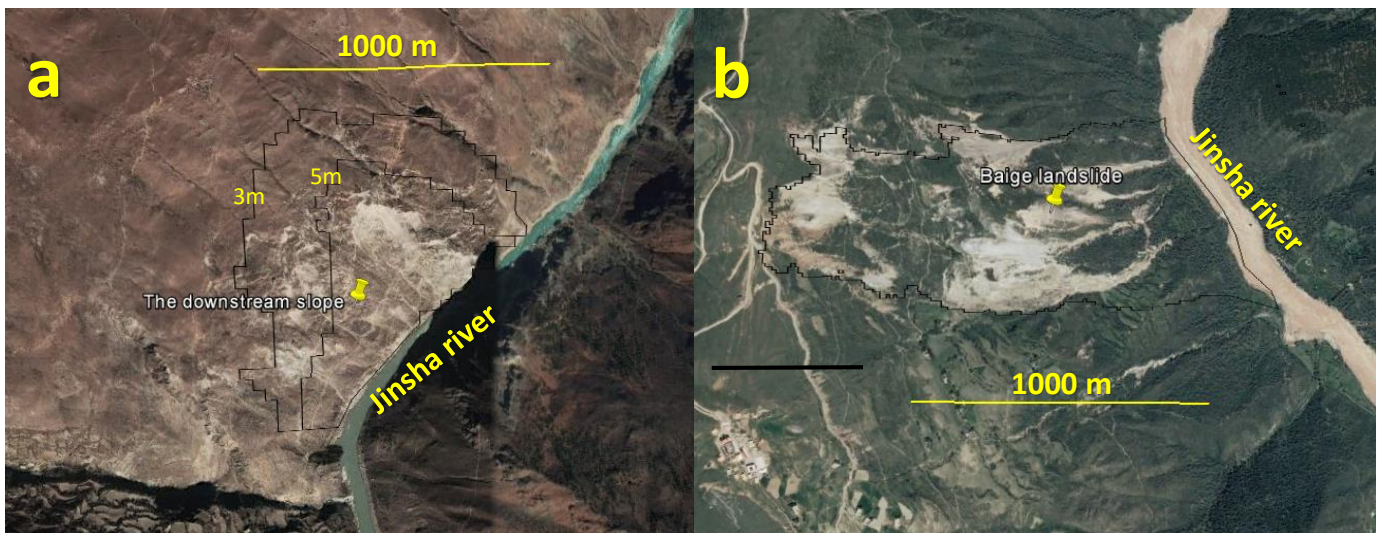
Figure 7: High spatial resolution images from the ©Google Earth. The image to the left is acquired on 30 March 2015 for the Mindu slope (a) and the right image is acquired on 18 July 2017 for the Baige slope (b).

23

510　**Table 1. List of 19 base images in early 2018 and 9 targeted images. Base images were used to detect slope displacements in targeted images. Image pairs used in this step are #3-#97.**

19 base images in the stable period (in early 2018)	5 target images in the moving period (in 2019)
January: 11, 13, 16, 23, 28	
February: 5, 12, 17, 25	
March: 4, 9, 14, 19, 29	2019: 13-Apr., 17-Jul., 24-Aug., 5-
April: 3, 16, 23	Oct., 12-Nov.
May: 21	
June: 5	

Table 2. Eight periods (image ~~pairs~~pair #98-#105) were used to derive the Mindu slope movement.

Image pairs	Base image	Target image
#~~1~~98	28 Oct. 2018	24 Nov. 2018
#~~2~~99	24 Nov. 2018	23 Jan. 2019
#~~3~~100	23 Jan. 2019	14 Mar. 2019
#~~4~~101	14 Mar. 2019	18 May 2019
#~~5~~102	18 May 2019	17 Jul. 2019
#~~6~~103	17 Jul. 2019	28 Sep. 2019
#~~7~~104	28 Sep. 2019	29 Nov. 2019
#~~8~~105	29 Nov. 2019	07 Feb. 2020

515　**Table 3. Detected image shifts (system error) in the "stable zone". The EW-std and NS-std indicates uncertainties of the method and the EW-mean and NS-mean were used to derive the final displacements in image ~~pairs~~pair #1 and #2.**

Image pairs	Dates	EW-mean	EW-std	NS-mean	NS-std	snr-mean	snr-std
#1	2015.11.13 2018.11.12	-0.495077	0.181026	-7.275188	0.253885	0.989819	0.001601
#2	2018.11.12 2019.11.12	4.115833	0.056559	9.914275	0.136149	0.989803	0.001434

520